A R C H I V E S O F M E T A L L U R G Y A N D M A T E R I A L S
Volume 55 2010 Issue 1

R. BOGUCKI*, S. M. PYTEL*

## THE FORMING OF HIGH MECHANICAL PROPERTIES OF LOW CARBON COPPER BEARING STRUCTURAL STEEL

## KSZTAŁTOWANIE WYSOKICH WŁASNOŚCI MECHANICZNYCH NISKOWĘGLOWEJ STALI KONSTRUKCYJNEJ Z DODATKIEM MIEDZI

The results of microstructure and mechanical properties of low-carbon copper bearing steel which is characterized by high yield strength equal to 900 MPa and minimum impact energy equal to 81J at low temperature (-84°C) are presented in this paper. The steel contains higher amount of nickel (6% wt.) and copper (2% wt.) as well as lower content of carbon (0,03% wt.) in comparison with grade HSLA-100 steels. High mechanical properties of the steel through appropriate selection of its chemical composition and heat treatment parameters were obtained. It was observed that hardening and then tempering in dual-phase range $\alpha+\gamma$ leads to formation of multiphase microstructure consisting of martensite laths, polygonal ferrite with precipitates of $\varepsilon\_Cu$ and retained austenite. This microstructure ensures high strength with good formability and resistance to brittle fracture.

*Keywords*: High Strength Low Alloy, copper addition, microstructure, mechanical properties, heat treatment

W pracy przedstawiono wyniki badań mikrostrukturalnych i wytrzymałościowych, niskowęglowej stali z dodatkiem 2% miedzi o granicy plastyczności $R_{p0,2}$ powyżej 900 MPa i pracy łamania na poziomie 81 J w temperaturze -84 °C. Badana stal charakteryzowała się podwyższona zawartością niklu (6% wag.) miedzi (2% wg.) oraz obniżoną koncentracją węgla (0,03% wg.) w porównaniu do klasycznej stali z gatunku HSLA 100. Wysokie własności mechaniczne zostały uzyskane poprzez sterowanie składem chemicznym oraz obróbką cieplną. Zaobserwowano, że hartowanie z następnym odpuszczaniem w zakresie dwufazowym $\alpha+\gamma$ prowadzi do utworzenia wielofazowej struktury składającej się z martenzytu listwowego, ferrytu poligonalnego z wydzieleniami fazy $\varepsilon\_Cu$ oraz austenitu szczątkowego. Mikrostruktura taka zapewnia wysokie własności wytrzymałościowe, dobrą plastyczności i odporność na pękanie.

## 1. Introduction

The heavy steel plates used for marine constructions [1-8] are a specific group of materials in which high mechanical properties and resistance to brittle fracture at low temperature as well as good weldability are strongly required. In 1981 the Naval Sea Systems Command (NAVSEA) initiated a research program to develop high-strength low-alloy steels [9]. HSLA 80 steel was prepared as first. According to ASTM A710 standard this steel was characterized by yield point from 552 MPa (80 ksi) to 690 MPa (100 ksi) and the impact resistance at temperature of -84°C (-120°F) equal to 81J [10]. The next step in the development of such grade of the steel was to increase its strength with the ductility unchanged. The HSLA 100 steel was designed and let to applications in 1990 [9, 10]. In both grades of these steels copper content was increased, while improving metallurgical quality by reduction of sulfur and phosphorus content [1]. Addition of copper in amount 1-2% to such grade of steels permits to decrease carbon content while maintaining high strength. After heat treatment consisting in hardening and tempering, the precipitation process of copper forms very small particles $\varepsilon\_Cu$ phase which caused increase of strength [1-7, 11].

In accordance with the military standard [10] the yield strength in the range of 690 MPa (100 ksi) to 890 MPa (130 ksi) and the impact resistance equal to 81 J at -84 °C in HSLA 100 steel should be obtained. At present, it is a basic structural steel used for sheathing and construction elements responsible for submarines, destroyers, aircraft carriers, as well as drilling platforms working at low temperatures.

The main goal of this investigation was to elaborate new grade of copper bearing steel which is characterized by high yield strength equal to 900 MPa and minimum

* INSTITUTE OF MATERIALS SCIENCE, CRACOW UNIVERSITY OF TECHNOLOGY, 31-864 KRAKÓW, UL. JANA PAWŁA II 37, POLAND

impact energy equal to 81J at low temperature (-84°C) through applying proper chemical composition and heat treatment.

## 2. Experimental procedure

The laboratory heat of about 220 kg weight was melted in vacuum-induction furnace. Chemical composition of the steel (W1) is shown in table 1.

TABLE 1

Chemical composition of the steels

| Grade of steel | Chemical composition, wt. % | | | | | | | | | | |
|---|---|---|---|---|---|---|---|---|---|---|---|
| | C | Mn | Si | Ni | Mo | Cu | P | S | Nb | Ti | Al |
| W1 | 0,03 | 1,97 | 0,24 | 5,80 | 0,95 | 2,11 | 0,005 | 0,003 | 0,05 | 0,10 | 0,021 |
| HSLA100[1] | 0,06 | 1,05 | 0,4 | 3,65 | 0,65 | 1,75 | – | – | – | – | – |

[1] – MIL-S-24645A/1991

In comparison with HSLA 100 steel, content of nickel in steel W1 was increased up to 6% and copper up to 2%, whereas content of carbon was restricted to 0,03%.

The thermomechanical processing was performed as shown in Fig. 1. In first stage of treatment the ingot was heated up to 1250°C and next rolling was carried out in temperature range from 1200°C to 1100°C with total reduction of δ=50%. Then slab was cooled in air to ambient temperature. In the second stage a conventional controlled rolling was applied. The ingot was heated below recrystalization temperature of austenite (up to 950°C) and rolled with reduction equal to δ=75%. As a result of rolling procedure plate with 25 mm thickness was obtained.

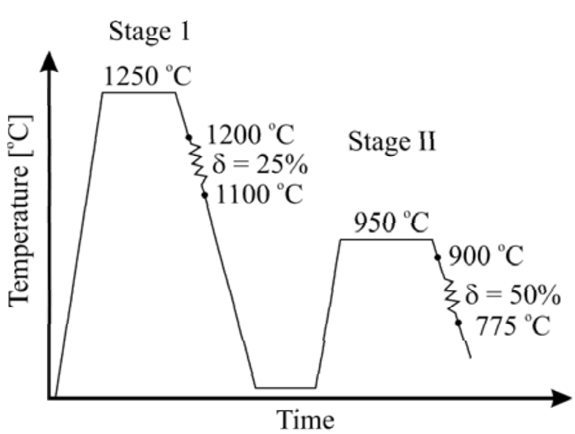


Fig. 1. Scheme of thermo mechanical processing

In order to determine a phase transformation temperature of the steel the measurement using dilatometer NETZSCH TASC 414/2 was carried out. The dilatometer analysis was conducted in argon atmosphere using cylindrical samples with 4 mm diameter and 25 mm length orientated transversely to rolling direction. The specimens were heated up to 950°C and then cooled at a rate of about 20°C/min.

The heat treatment of the steel consisted in austenitizing at 900 °C for one hour and then quenching in water. Next samples were tempered in the temperature range from 450 to 800°C for one hour (with step 25°C within), followed by quenching in water.

Tensile test was performed in accordance with EN 10002-1:2001 at room temperature using the specimens prepared transversely to the rolling direction of the plate. For each tempering temperature two cylindrical specimens with 5 mm diameter and 25 mm gauge length were prepared. The test was carried out on the 20 EU hydraulic testing machine. Impact test was conducted by means of standard Charpy V-notch specimens using impact testing hammer with initial energy of 300 J. The impact energy was determined at an ambient (25 °C) and subzero (-84 °C) temperatures.

Microstructure examinations of the tempered samples were conducted using scanning electron microscope (SEM) JOEL JSM5510LV. Observations were carried out on longitudinal sections of metallographic specimens etched in 4% nital.

A detailed assessment of microstructure for selected specimens characterized by the highest mechanical properties was carried out using Philips CM 20 transmission electron microscopy (TEM). Thin foils were prepared in a jet-polishing Struers TenuPol-5 using a 30% solution of nitrous acid in ethanol at -50 °C. Identification of observed phases was carried out by indexed selected area diffraction (SAD) pattern. Interplanar distances were determined by diffraction program and next crystallographic plane type was defined.

## 3. Results

### 3.1. Dilatometer examination

The start and finish of austenite transformation temperature was determined as 668°C and 813°C respectively. The beginning and end of bainitic transformation was observed sequentially at 353°C and 216°C. Fig. 2 shows the change of linear expansion of sample as a function of temperature.

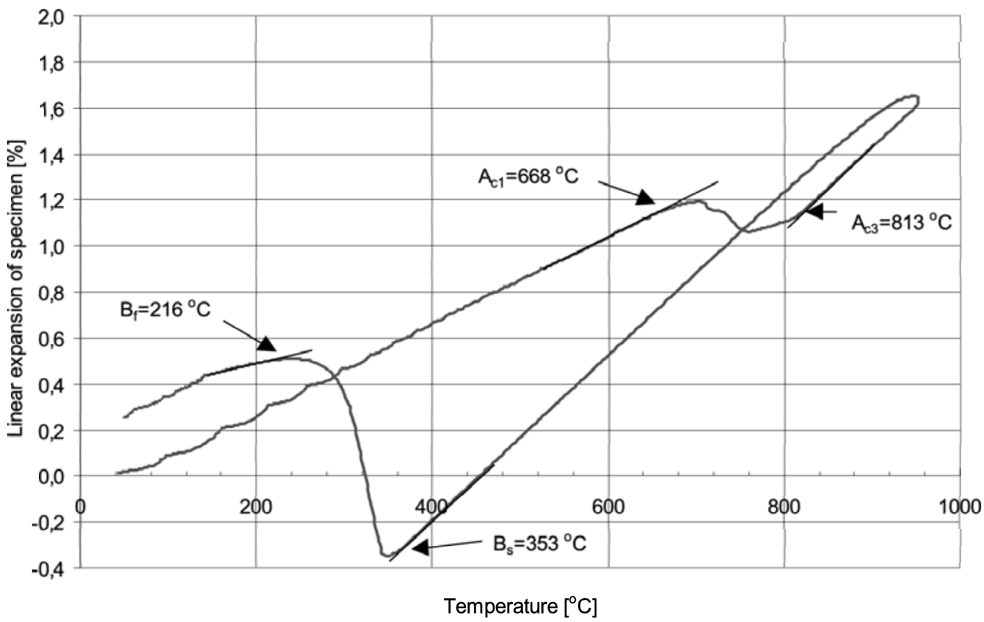


Fig. 2. Linear expansion of the dilatometer sample as a function of temperature

### 3.2. Mechanical properties

The course of the mechanical properties of the steel as a function of the tempering temperature is shown in Fig. 3.

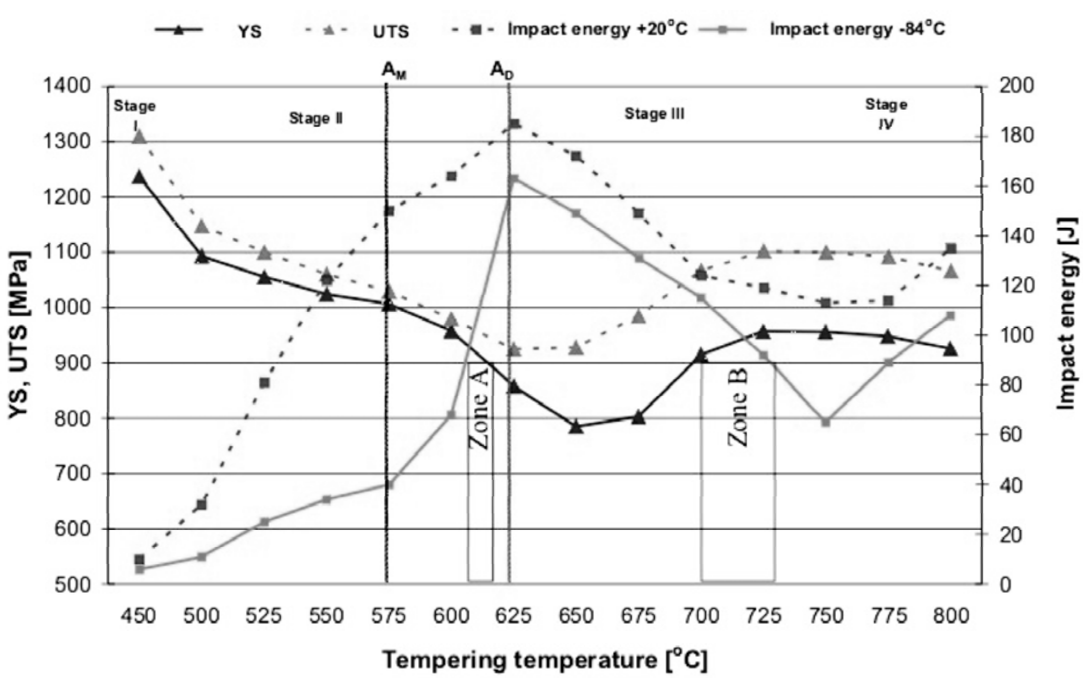


Fig. 3. Course of yield strength, ultimate tensile strength and impact energy at 20°C and -84°C as a function of tempering temperature where: $A_M$ – ferrite to austenite transformation temperature defined on the basis of microstructure, $A_D$ – ferrite to austenite transformation temperature defined on the basis of dilatometer test

The results presented in Fig.3 show a typical tempering behavior for Cu-bearing steel. Maximum strength (YS =1237 MPa and UTS =1310 MPa) and low impact energy equal to 10J at ambient temperature and 6J at -84°C were obtained after tempering at 450°C. The increase of tempering temperature causes the drop of strength and growth of impact energy. The maximum impact energy equal to 185 J was obtained after tempering at temperature 625°C, whereas the minimum strength amounted to 785 MPa at temperature 650°C. The further increase of tempering temperature caused drop of impact resistance which reached next minimum at 750°C while the strength increased to 957 MPa at 725°C. The criterion of minimum yield strength above 900 MPa and minimum impact resistance equal to 81 J at -84 °C was obtained after tempering in the narrow range of temperature above 600 °C (zone A) and in a wider temperature range 700-725 °C (zone B)-Fig. 3. For comparison purposes the average values of mechanical properties are presented in Table 2.

TABLE 2

Mechanical properties of the steel after different tempering temperature

| W1 steel | | $YS_{0,2}$ | UTS | EL | RA | Impact energy 20°C | Impact energy -84 °C |
|---|---|---|---|---|---|---|---|
| | | MPa | | % | | J | |
| Tempering temperature, °C | 450 | 1237 | 1310 | 13,9 | 49,6 | 10 | 6 |
| | 500 | 1093 | 1148 | 14,6 | 63,4 | 32 | 11 |
| | 525 | 1055 | 1100 | 15,4 | 64,9 | 81 | 25 |
| | 550 | 1024 | 1060 | 15,9 | 65,3 | 122 | 34 |
| | 575 | 1007 | 1029 | 17,2 | 68,3 | 150 | 40 |
| | 600 | 958 | 980 | 18,0 | 70,2 | 164 | 68 |
| | 625 | 858 | 925 | 18,6 | 69,6 | 185 | 163 |
| | 650 | 785 | 928 | 18,2 | 68,7 | 172 | 149 |
| | 675 | 803 | 985 | 17,4 | 67,0 | 149 | 131 |
| | 700 | 915 | 1067 | 17,1 | 65,4 | 124 | 115 |
| | 725 | 957 | 1102 | 17,3 | 62,7 | 119 | 92 |
| | 750 | 956 | 1100 | 17,8 | 66,3 | 113 | 65 |
| | 775 | 948 | 1092 | 18,1 | 67,1 | 114 | 89 |
| | 800 | 926 | 1066 | 18,1 | 68,3 | 135 | 108 |

**Microstructure**

Microscopic observations by SEM revealed slight differences in microstructures of samples tempered in temperature range of 450-575°C, Fig. 4a-c. To 575°C microstructure was characterized by similar morphology consisting of tempered martensite and bainite. Significant changes of the microstructure were observed when $\alpha \rightarrow \gamma$ transformation started at temperature 600°C, Fig. 4d. Application of intercritical annealing temperature (in range $\alpha \rightarrow \gamma$) and subsequently cooling the samples in water caused formation of a multi phase structure (ferrite + martensite + austenite) with a growing volume of martensite, Fig. 4e. At temperature 800°C after cooling in water the microstructure of martensite – bainite was observed, Fig 4f.

TEM analysis of the tempered specimen at 625 °C, where there is a sudden increase of impact energy, revealed a small amount of new retained austenite presented at the martensite lath boundaries. The austenite was rich in alloying elements (Ni and Cu) and stable even after cooling in water, Fig. 5a. A selected area of diffraction pattern from new retained austenite is shown in Fig. 5b. The very fine spherical precipitates of $\varepsilon\_Cu$ which have diameters ranging from 10 to 40 nm were observed simultaneously, Fig. 6a. A selected area of diffraction pattern from $\varepsilon\_Cu$ particles is shown in Fig. 6b. Increase of temperature to 700 °C leads to the impoverishment of austenite in alloying elements. The packages new martensite laths 100-200 nm wide was formed after cooling, Fig. 7a. Areas of polygonal ferrite and small particles of $\varepsilon\_Cu$ which have diameters of 10-50 nm were also found, Fig. 7b. After tempering at 750 °C the microstructure consisted of martensite laths with a width of 500 nm and areas characterized by low dislocation density were observed locally, Fig. 8a. The increased volume of retained austenite causes a decrease in the amount of alloying elements present in it. As a result of cooling the microstructure consists of mixture of martensite laths and bainite, Fig. 8b.

## 4. Discussion

The increase of strength and drastic drop of impact energy of the tempered steel at 450°C is associated with the beginning of fine particles ($\varepsilon\_Cu$) precipitation. In the early stage (I) of precipitation this phase creates coherent

clusters which are *Guinier-Preston* (*GP*) zones with crystallographic structure which is the same as matrix [1, 12].
The influence of the dislocations with forming GP zones consists in a shearing of particles by dislocations in accordance with the Friedel mechanism [13, 14]. As a result, the leaps are formed in GP zones. They lead to strengthening of matrix and sudden decrease of the crack resistance. Direct observation of GP zones is difficult because of the high dislocation density and low stress contrast around these areas.

The increase of the tempering temperature above 450°C causes a systematic drop of strength with simultaneous increase of impact energy, which corresponds to stage II. At room temperature systematic increase of impact strength was observed.
Sudden increase of impact resistance at low temperature was observed at the moment of appearance of $\alpha \rightarrow \gamma$ transformation, Fig. 4d, as shown by broken line $A_{c1}$ in graphs, Fig. 3. Stable austenite at ambient temperature is responsible for the results. It forms on boundary of tempered martensite laths, Fig. 5. It presents strong barriers to the propagation of brittle cracking.

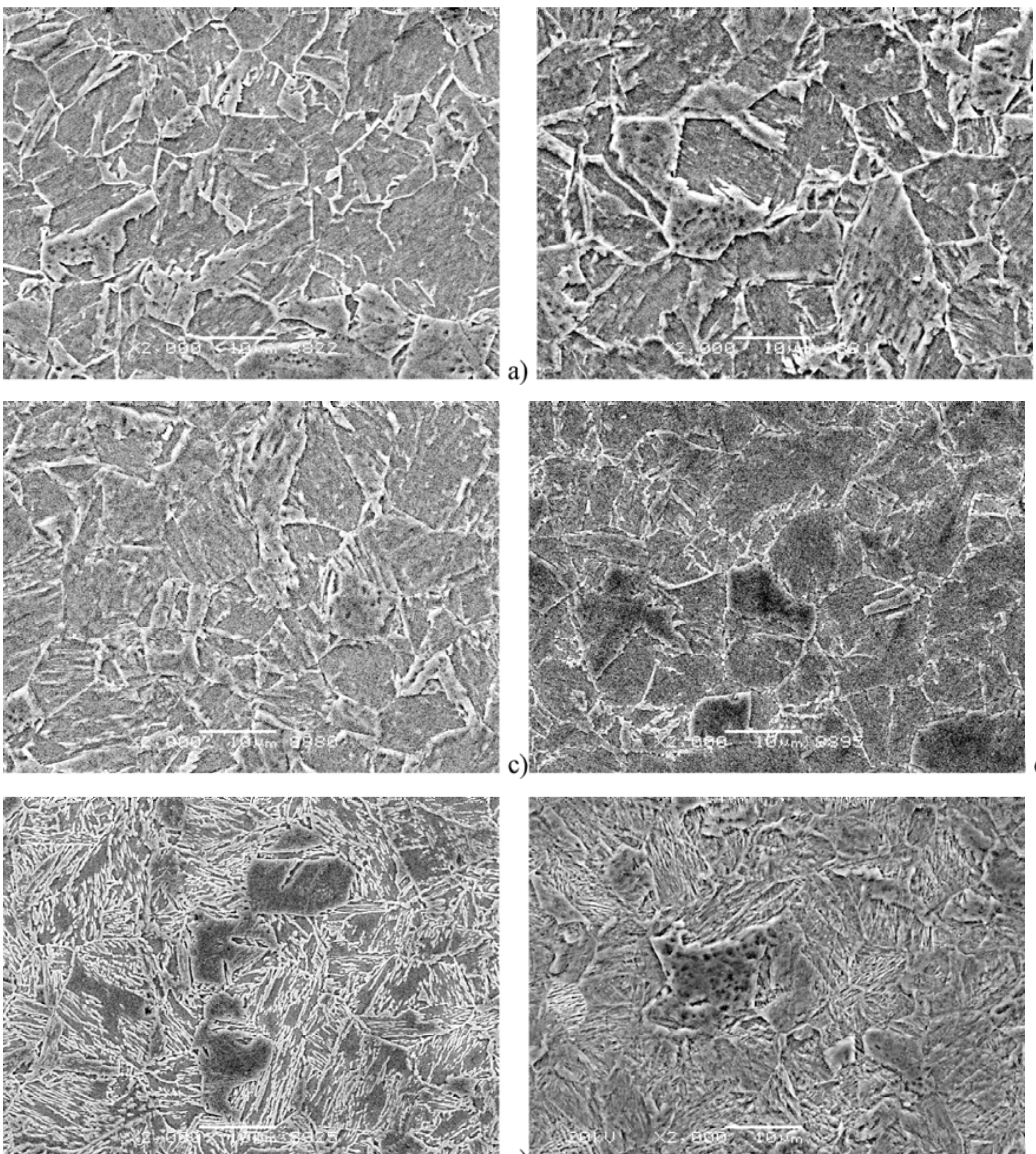

a) b) c) d) e) f)

Fig. 4. SEM micrographs of the steel after tempering at temperatures: a) 450 °C, b) 500 °C ,c) 575 °C d) 600 °C, e) 650 °C f) 800 °C

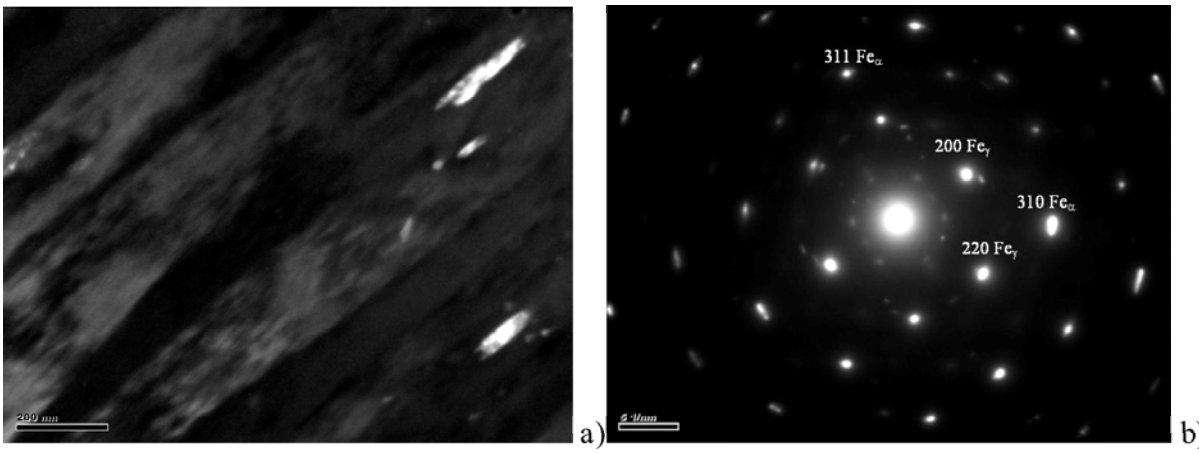


Fig. 5. TEM micrographs of the steel after tempering at 625 °C: a) dark field images showing tempered martensite laths region with retained austenite at lath boundaries; b) SAD pattern and index of SAD pattern identifying retained austenite

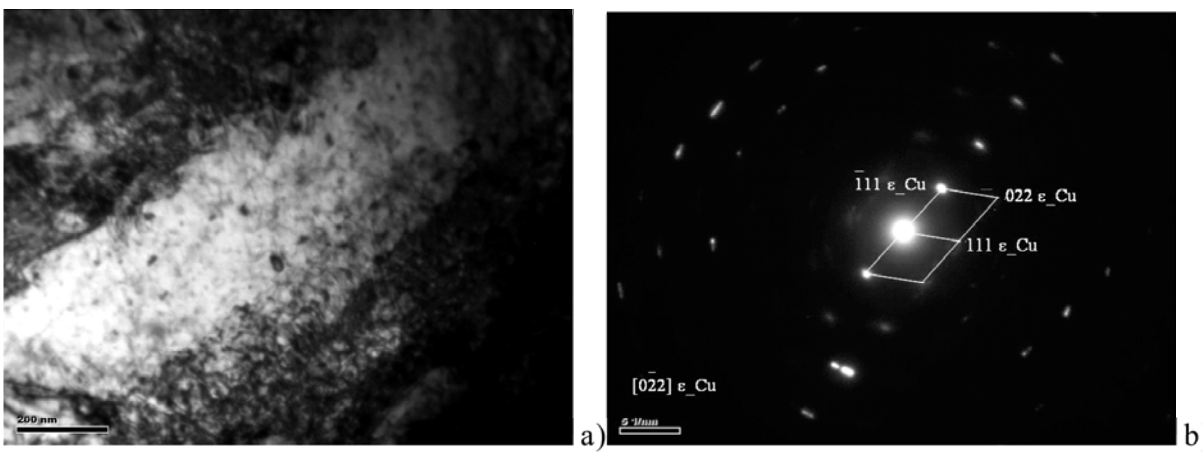


Fig. 6. TEM micrographs of the steel tempered at 625°C: a) BF images showing recovered martensite lath with of ε_Cu precipitates; b) SAD pattern and index of SAD pattern identifying precipitates Cu

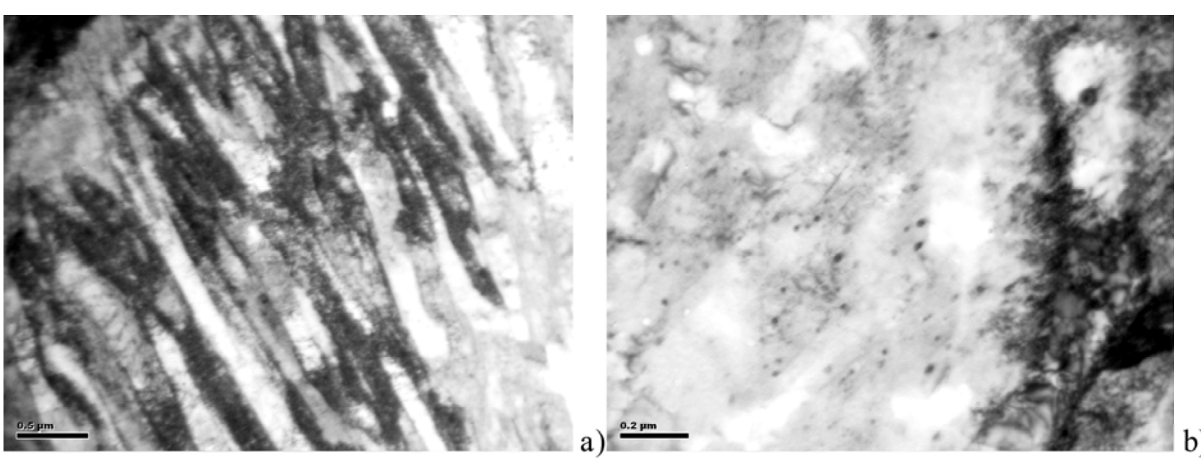


Fig. 7. TEM micrographs of the steel tempered at 700°C: a) new laths martensite after cooling in water; b) area of polygonal ferrite with of ε_Cu precipitates – BF images

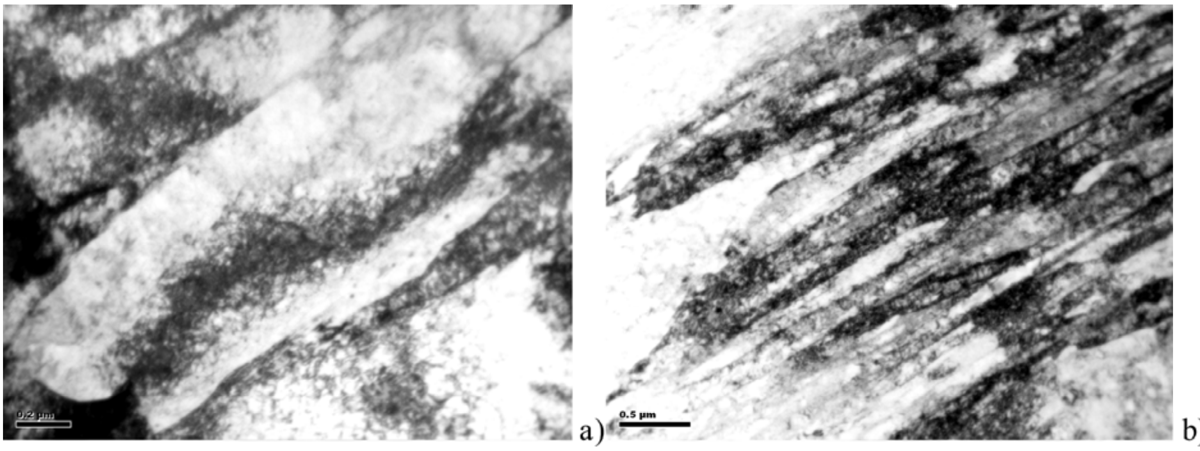


Fig. 8. TEM micrographs of the steel tempered at 750 °C: a) area of bainite with low density dislocations; b) area of mixed martensite and bainite laths formed with retained austenite after cooling in water – BF images

The maximum of impact energy for the steel tested at temperature of -84 °C was observed for samples tempered at 625 °C. Observed systematic drop of strength is caused by decomposition of martensite matrix and less strengthening by Orowan mechanism, which results from the increase of precipitations and distance between particles of ε_Cu phases.

Subsequent increase of the tempering temperature caused the decrease of impact resistance with simultaneous increase of the strength, which corresponds to stage III. With the increase of the tempering temperature, volume fraction of retained austenite increases with simultaneous decrease of its thermal stability caused by a reduction of the amount of alloying elements. Annealing in intercritical range $\alpha+\gamma$ with subsequent accelerated cooling caused the formation of a mixture of newly formed martensite lath and polygonal ferrite with ε_Cu precipitations, Fig. 7. The result is sudden decrease of impact energy at temperature of -84 °C joined with the increase of strength.

At the tempering temperature of 750°C another minimum of impact resistance at -84°C appeared. Microscope observations carried out at this temperature revealed laths structure with different dislocation density. Dissolving ε_Cu phase particulates in austenite and such elements as Ni, Mo locally increases its heterogeneity, leading to the formation of a mixed structure of bainite and martensite laths, Fig. 8a and b.

## 5. Conclusions

The required level of mechanical properties such as yield strength YS=900 MPa and impact energy equaling 81 J at -84°C was met in two temperature ranges. Analyzing mechanical properties course, the first distinguished narrow temperature range at which the above conditions were met was 600°C (zone A). But from the technological point of view carrying out heat treatment in such a narrow temperatures range especially in the case of plates would be very difficult or just impossible to execute.

The second area where these standard requirements were met occurred in the range of tempering temperature of 700-725°C (zone B). Observed microstructure in this zone was a mixture of newly formed low-carbon martensite laths and areas of polygonal ferrite with precipitation of ε_Cu phase. Martensite laths formed from the retained austenite were characterized by a smaller width of about 100-200 nm.

REFERENCES

[1] A. K. Lis, Podstawy kształtowania wysokiej odporności na pękanie ultraniskowęglowych stali bainitycznych – monografia 53, Wydawnictwo Politechniki Częstochowskiej, Częstochowa 1998.

[2] S. J. Mikalac, M. G. Vassilaros, Strength and toughness response to aging in a high copper HSLA-100 steel – Proceeding of the International Conference on Processing, Microstructure and Properties of Microalloyed and oder Modern High Strength Low Alloy Steels, June 3-6 1991. Pittsburgh PA, USA, 331-343.

[3] M. Blicharski, C. I. Garcia, S. M. Pytel, Structure and Properties of ULCB Steels for Heavy Section Applications, Proceedings of International Symposium on Processing, Microstructure and Properties of HSLA Steels, October 1987, Pittsburgh, PA, USA.

[4] R. P. Foley, M. E. Fine, Microstructure and property investigation of quenched and tempering HSLA-100 steel, Processing, Microstructure and Properties of Microalloyed and Other Modern High Strength Low Alloy Steels, Pittsburgh, PA, June 3-6, 315-330, 1991 Pittsburgh, PA.

[5] S. Panwar, D. B. Goel, O. P. Pandy, K. S. Prasad, Aging of copper Bering HSLA-100 steel, Bull. Mater. Sci. **26**, 4, 441-447, June 2003.

[6] S. K. Dhua, A. Ray, D. S. Sarma, Effect of tempering temperatures on the mechanical properties and microstructures of HSLA-100 type copper-bearing steels – Materials Science and Engineering **A318**, 197-210 (2001).

[7] R. Bogucki, K. Miernik, S. M. Pytel, Influence of molybdenum addition on microstructure-property relationship of copper Bering high strength low alloy steel, mat. konf. New trends in technology system operation, Presov Slovak Republic 20-21 October 2005.

[8] H. Bugłacki, Analiza właściwości mechanicznych i spawalności stali wysokiej wytrzymałości na konstrukcje oceanotechniczne i okrętowe, monografia 23, Politechnika Gdańska, Wydawnictwo Politechniki Gdańskiej, Gdańska 2001.

[9] T. W. Montemarano, B. P. Sack, J. P. Gudas, M. G. Vassilaros, H. H. Vanderveldt, High strength low alloy steels in naval construction, Journal of Ship Production, **2**, 3, 145-162, August 1986.

[10] MIL-S-24645A(SH), Military Specyfication, Steel Plate, Sheet, or Coil, Age-Hardening Alloy, Structural, High Yield Strength (HSLA-80 and HSLA 100), January 1991.

[11] S. M. Pytel, R. Bogucki, Wpływ jakości metalurgicznej na mechaniczne właściwości stali konstrukcyjnej HSLA 100 z dodatkiem miedzi, mat. konf.: III Konferencja Naukowa "Współczesne zagadnienia w materiałoznawstwie i technologii bezwiórowej" Bydgoszcz 2001.

[12] M. Mujahid, A. K. Lis, C. I. Garcia, A. J. DeArdo, Structure – properties studies of Cu-containing HSLA 100 steel, Processing, Microstructure and Properties of Microalloyed and Other Modern High Strength Low Alloy Steels, 345-357. Pittsburgh, PA, June 3-6, 1991, Pittsburgh, PA.

[13] B. Reppich, Particle strebgthening, (w:) Materials science and technology, A comprehensive treatment, vol. 6, Plastic deformation and fracture of materials, Weinheim, VCH, 311-367 (1993).

[14] B. D. Wirth ed al, Multiscale modeling of radiation damage accumulation in bcc and fcc metals in the fusion environment, ICFRM-11, Kyoto Japan.

*Received: 10 September 2009.*